

Antiferromagnetic states of charge carriers in the ferromagnetic semiconductors $\text{CuCr}_2\text{S}_{4-x}\text{Se}_x$ ($0.5 \leq x \leq 1.5$) with Curie points above room temperature

L. I. Koroleva

M. V. Lomonosov Moscow State University, 119899 Moscow, Russia
(Submitted 18 March 1994)

Zh. Eksp. Teor. Fiz. **106**, 280–296 (July 1994)

A semiconductor type of conduction has been discovered in $\text{CuCr}_2\text{S}_{4-x}\text{Se}_x$, which is a solid solution of the two ferromagnetic chalcogenide spinels CuCr_2S_4 and CuCr_2Se_4 with a metallic type of conduction, when $0.5 \leq x \leq 1.5$. The semiconducting samples exhibit decreased values of the magnetic moments, the Curie points, and the anomalous Hall effect in comparison with the extreme compounds. The paramagnetic susceptibility of all the samples obeys the Curie–Weiss law, the paramagnetic Curie temperature θ_p being below the Curie temperature T_C . A large blue shift of the absorption edge (~ 0.15 eV), which is associated with ferromagnetic ordering, has been discovered for the semiconducting samples, allowing the existence in them of antiferromagnetic microregions (microregions with disrupted ferromagnetic ordering created by the self-trapping of charge carriers in them due to a gain in the energy of interband s – d exchange). A calculation has shown that the decreased values of the magnetic moment in the semiconducting samples are attributable to the existence of antiferromagnets including three or four Cr^{3+} ions near selenium ions.

1. INTRODUCTION

When the two ferromagnetic spinels CuCr_2S_4 and CuCr_2Se_4 with a metallic type of conduction¹ were mixed, it was unexpectedly found that the samples with $0.5 \leq x \leq 1.5$ in $\text{CuCr}_2\text{S}_{4-x}\text{Se}_x$ have a semiconductor type of conduction.² Their magnetic properties also exhibit some peculiarities: decreased values of the Curie temperature T_C , the paramagnetic Curie temperature θ_p , and the magnetic moment per formula unit $n_{4.2\text{K}}$ in comparison with the extreme compounds of this system CuCr_2S_4 and CuCr_2Se_4 are observed. It was found that these semiconducting samples are characterized by a large blue shift of the absorption edge, which is associated with long-range magnetic ordering.³ The occurrence of such a blue shift allows the existence in them of antiferromagnetic microregions (regions with disrupted ferromagnetic ordering due to a gain in the energy of interband s – d exchange).⁴

This article has the following structure. After the introduction, the magnetic properties will be described in Sec. 2, and the electrical properties of the $\text{CuCr}_2\text{S}_{4-x}\text{Se}_x$ system of solid solutions will be described in Sec. 3. Data from optical investigations of semiconducting samples will be presented in Sec. 4. Then it will be shown in Sec. 5 on the basis of an analysis of the crystal structure of a copper spinel simultaneously containing S and Se that antiferromagnetic states of charge carriers can form around Se ions. It follows from the calculation performed in Sec. 5 that the underestimated magnetic moments of the semiconducting samples are attributable to the existence of antiferromagnets, each of which contains three or four Cr^{3+} ions that are nearest neighbors of selenium ions.

2. MAGNETIC PROPERTIES OF THE $\text{CuCr}_2\text{S}_{4-x}\text{Se}_x$ SYSTEM OF SOLID SOLUTIONS

The magnetization σ was measured by the ballistic method in fields H up to 55 kOe at $T = 4.2$ K and in fields

up to 14 kOe at $77 \leq T \leq 450$ K. The plots of $\sigma(H)$ for all the samples investigated rapidly reach saturation both at 4.2 K and in the temperature range investigated from 77 K to the vicinity of T_C . Thus, saturation is nearly achieved in a 10 kOe field. The value of T_C was determined both by extrapolating the steepest part of the plot of $\sigma(T)$ to the temperature axis and by the Belov–Arrott method of thermodynamic coefficients. The paramagnetic susceptibility was measured by a weighing method with electromagnetic compensation. The paramagnetic susceptibility of all the samples studied obeys the Curie–Weiss law, the values of θ_p and T_C for each sample being close, as is typical of ferromagnets.

Figure 1 presents plots of the magnetic moment (in μ_B per formula unit) as a function of x for the $\text{CuCr}_2\text{S}_{4-x}\text{Se}_x$ system. The magnetic moment was determined in two ways: from the magnetization at 4.2 K in a 50 kOe field ($n_{4.2\text{K}}$) and from data on the paramagnetic susceptibility (n_p , which is calculated from the Curie constant C_M in the Curie–Weiss law). This figure also presents plots of the dependence of T_C and θ_p on the composition. As is seen from Fig. 1, all four plots have a minimum for the sample with $x = 1$.

3. ELECTRICAL PROPERTIES OF THE $\text{CuCr}_2\text{S}_{4-x}\text{Se}_x$ SYSTEM

The resistivity ρ was measured by the four-probe method, and the Hall emf was measured by the compensation method at a constant current. The plots of the dependence of the Hall resistivity $\rho_x = (U_x d)/I$ on the magnetic induction B were used to calculate the normal Hall coefficient, and the anomalous Hall resistivity ρ_x^a was determined with the aid of the known relation

$$\rho_x = R_0 B + \rho_x^a \quad (1)$$

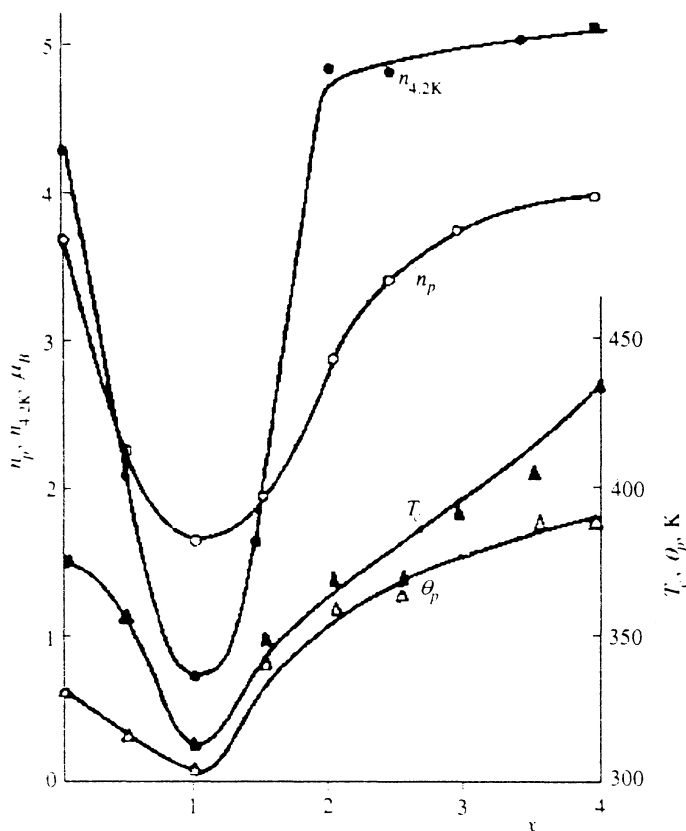


FIG. 1. $\text{CuCr}_2\text{S}_{4-x}\text{Se}_x$ system. Dependence of the magnetic moment per chemical formula unit at 4.2 K $n_{4.2\text{K}}$, the magnetic moment per chemical formula unit determined from the Curie-Weiss constant n_p , the Curie point T_C , and the paramagnetic Curie temperature θ_p on the composition.

Here U_H is the Hall emf, I is the current through the sample, and d is the dimension of the sample in the direction of the magnetic field. According to our measurements, the transverse magnetoresistance of all the samples was extremely small, less than $10^{-3}\%$. This created favorable conditions for measuring the Hall effect. The hole character of the charge carriers was determined from the sign of the thermoelectric power at room temperature. The concentration of the holes p and their mobility μ were calculated from R_0 and ρ .

Figure 2 presents plots of the temperature dependence of ρ , R_0 , p , and μ for $\text{CuCr}_2\text{S}_3\text{Se}$. The figure reveals that the conduction of this sample has a semiconductor character. The temperature dependence of these parameters of the samples with $x=0.5$ and 1.5 is very similar to that shown in Fig. 2. The dependences of R_0 , p , and μ on x at 100 K are presented in Fig. 3. The plots of $\rho_x^a(T)$ have a broad maximum below the Curie point, and the anomalous Hall effect nearly vanishes as T_C is approached. Figure 4 presents the dependence of the height of this maximum on x , which reveals that the anomalous Hall effect is virtually absent to within the accuracy of the experiment for the sample with $x=1$ and increases sharply as the concentration of holes increases. It is also observed for samples with a metallic type of conduction. The smallness of ρ_x^a in the semiconducting samples of this system is consistent with the conclusions of Ref. 5, where it was shown that the ratio between the constants of the anomalous and normal Hall effects in several orders of magnitude lower in magnetic semiconductors than in metals.

The conduction of the samples with $x \geq 2$ and $x=0$ has

a metallic character. As Fig. 3 reveals, μ and p scarcely vary with the composition in the samples with $x \geq 2$. The data on the magnetic and electrical properties of the $\text{CuCr}_2\text{S}_{4-x}\text{Se}_x$ system of solid solutions are presented in Table I. This table also gives the lattice constants. It is seen that the lattice constant varies linearly with x in this system, pointing out its high solubility.

As is seen from Figs. 1-4 and Table I, the samples with $x=0.5$, 1 , and 1.5 are of greatest interest. They are ferromagnetic semiconductors with Curie points above room temperature (355, 310, and 350 K, respectively). As the temperature rises, ρ and μ drop, and p increases with an activation energy that varies with the temperature (Table I and Fig. 2). At the same time, just these samples exhibit abrupt decreases in the magnetic moment, the Curie temperature, and the height of the maximum of ρ_x^a in comparison to the samples with $x=0$ and $x \geq 2$.

4. OPTICAL PROPERTIES OF SEMICONDUCTING SAMPLES IN THE $\text{CuCr}_2\text{S}_{4-x}\text{Se}_x$ SYSTEM OF SOLID SOLUTIONS

Since the samples of this system were polycrystalline, diffuse reflectance spectroscopy was employed to investigate their optical properties. This method is more suitable for investigating polycrystalline samples than is specular reflection spectroscopy, since the reflected light from the surface of a powdered sample, rather than a polished surface, is investigated in this case. Polishing is known to frequently alter the properties of a surface and introduce various contaminants. A novel system, which was described in Ref. 6, was assembled to investigate the diffuse

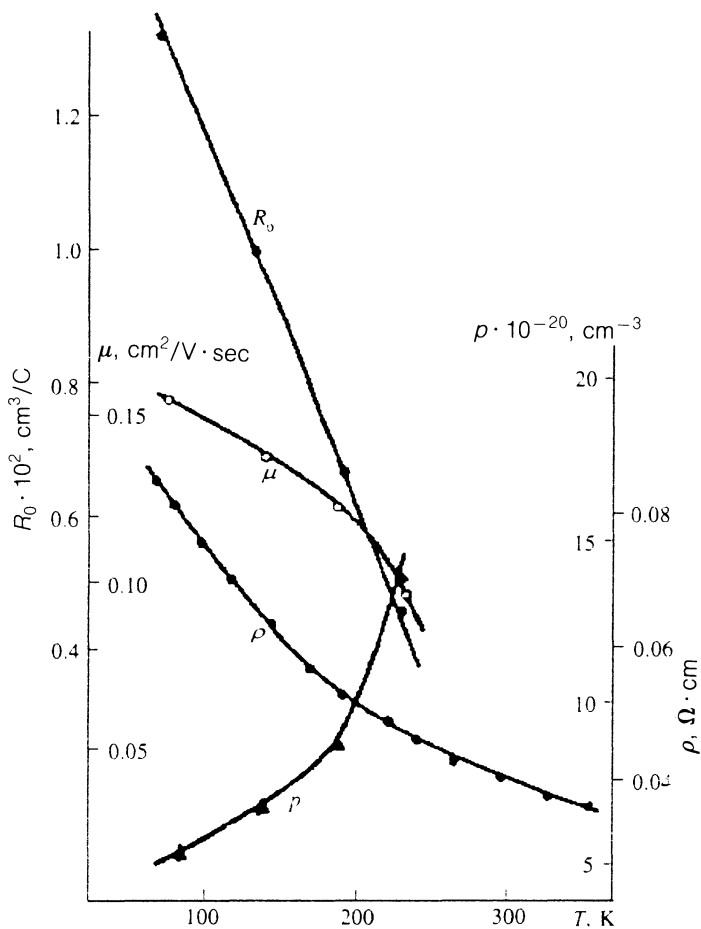


FIG. 2. Temperature dependence of the normal Hall constant R_0 , the resistivity ρ , the mobility μ , and the concentration of charge carriers p for $\text{CuCr}_2\text{S}_3\text{Se}$.

reflectance spectra. The diffuse reflectance measurements were performed according to a single-beam scheme with alternating measurements of the sample and the reference. The optical part of the system was designed in such a manner that the intensity of the light reflected from the surface of crystallites in a powdered sample at angles not exceeding 6.2° is recorded. This ensures satisfaction of the

condition for applying the computationally convenient Kramers–Kronig relations, which were used to calculate the spectra of the absorption coefficient α and the refractive index n from the diffuse reflectance spectra. The Kramers–Kronig calculation method described in Ref. 7 was used. The experimental data were reduced and the spectra of α and n were calculated on ES-1010 and Iskra 1030 M computers using specially developed programs.

The diffuse reflectance spectra were investigated for the same samples on which the magnetic and electrical properties described in Secs. 2 and 3 were measured. A pronounced absorption edge was discovered in the samples

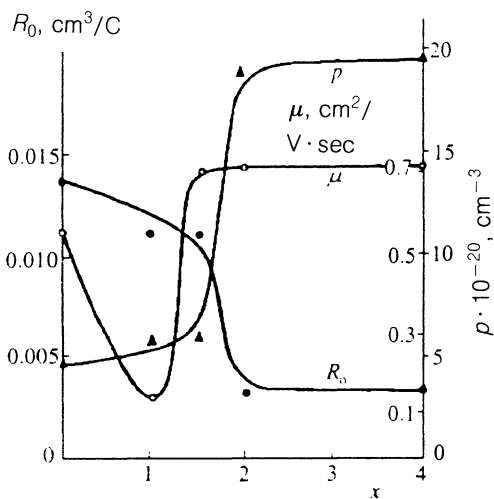


FIG. 3. Dependence of the normal Hall constant R_0 , the mobility of μ , and the concentration of charge carriers p on the composition in the $\text{CuCr}_2\text{S}_{4-x}\text{Se}_x$ system at 100 K.

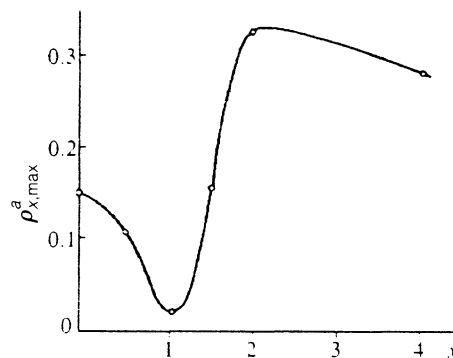


FIG. 4. Dependence of the maximum anomalous Hall resistivity $\rho_{x,\text{max}}^a$ of the $\text{CuCr}_2\text{S}_{4-x}\text{Se}_x$ system on the composition.

TABLE I. Characteristics of the $\text{CuCr}_2\text{S}_{4-x}\text{Se}_x$ system of solid solutions.

x	$a, \text{\AA}$	T_C, K	θ_p, K	$n_{4.2\text{K}}, \mu_B$	n_p, μ_B	Type of conduction	p, cm^{-3} (100 K)	$\mu \text{ cm}^2/\text{V} \cdot \text{sec}$ (100 K)
0	9.813	377	335	4.32	3.72	metallic	$5 \cdot 10^{20}$	0.55
0.5	9.880	355	—	1.90	2.08	semiconductor	—	—
1.0	9.940	310	302	0.75	1.68	semiconductor	$6 \cdot 10^{20}$	0.15
1.5	10.021	350	341	1.8	1.96	semiconductor	$6 \cdot 10^{20}$	0.70
2.0	10.075	369	362	4.8	2.88	semiconductor	$1.9 \cdot 10^{21}$	0.70
2.5	10.137	370	369	4.8	3.44	metallic	—	—
3.0	10.197	392	381	5.0	3.72	metallic	—	—
3.5	10.262	406	390	5.0	3.72	metallic	—	—
4.0	10.334	437	388	5.08	3.92	metallic	$2 \cdot 10^{21}$	0.70

Here a is the lattice constant; T_C is the Curie point; θ_p is the paramagnetic Curie point; $n_{4.2\text{K}}$ is the magnetic moment per chemical formula unit measured at 4.2 K, n_p is the magnetic moment per chemical formula unit, which is equal to the product of the g factor and twice the spin of the chromium ion calculated from the Curie constant in the Curie-Weiss law; p is the concentration of holes; μ is the mobility of the holes.

with $x=0.5, 1.0,$ and $1.5,$ which have a semiconductor type of conduction. This provides further evidence that these samples are semiconductors. The special features of the spectra of the remaining samples with a metallic type of conduction are masked by these strong scattering of light by free charge carriers. The spectra of α of the samples with $x=0.5, 1.0,$ and 1.5 at $T=300$ K are shown in Fig. 5. As is seen from the figure, the absorption coefficients of these samples increase rapidly as the incident photon energy E increases from 0.8 eV to $E=3$ eV (the range of energies investigated), attesting to an absorption edge. The plots of $\alpha(E)$ have a characteristic form with a step and are reminiscent of the spectra of the ferromagnetic semiconductor CdCr_2S_4 (Refs. 8 and 9), where a large blue shift of the absorption edge associated with ferromagnetic

ordering was first discovered. The position of the absorption edge was determined from the maximum of n , as recommended in Ref. 10. At room temperature the absorption edge of the samples with $x=0.5$ and 1.0 is located at 1.1 eV. In the sample with $x=1.5,$ the edge is indistinct, since this sample is probably a translational phase between the semiconducting sample with $x=1.0$ and the metallic sample with $x=2.0$ (Fig. 3).

Figure 6 presents the spectra of α and n for the sample with $x=0.5$ at three temperatures. Curves 1 and 2 refer to temperatures below the Curiepoint $T_C,$ and curves 3 refer to the temperature range above $T_C.$ The spectra of α and n for the sample with $x=1$ have approximately the same character. The form of the plots of $\alpha(E)$ in Fig. 6 clearly indicates that the absorption band edge corresponding to

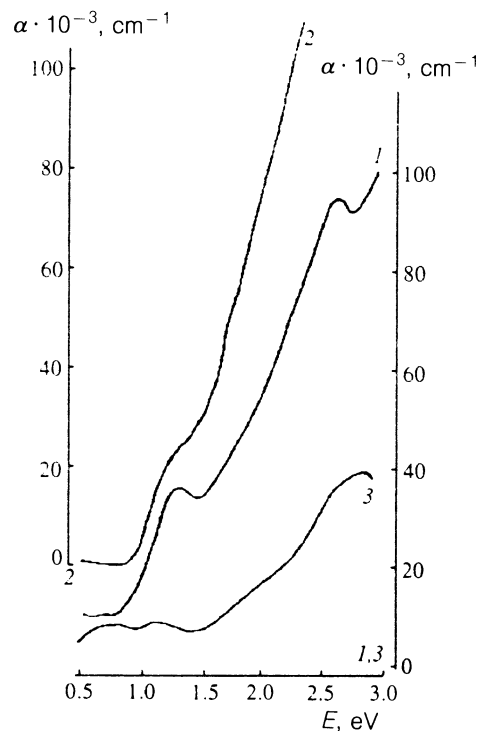


FIG. 5. Spectra of the absorption coefficient α of the $\text{CuCr}_2\text{S}_{4-x}\text{Se}_x$ system at room temperature for various values of x : 1—0.5; 2—1; 3—1.5.

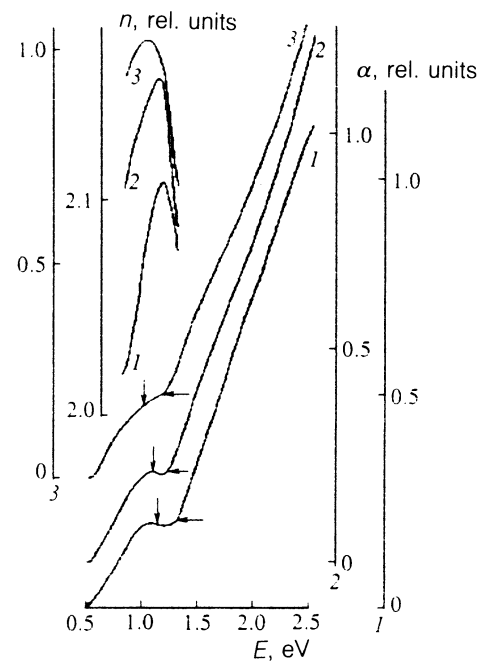


FIG. 6. Sample of $\text{CuCr}_2\text{S}_{3.5}\text{Se}_{0.5}.$ Spectra of the absorption coefficient α (three lower curves) and the refractive index n (three upper curves) at various temperatures (K): 1—210; 2—291; 3—406. The vertical arrows indicate the positions of the maxima on the $n(E)$ curves, and the horizontal arrows indicate the beginning of the sharp rise on the $\alpha(E)$ curves.

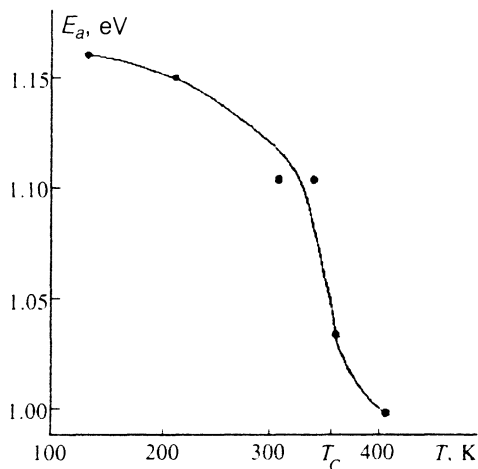


FIG. 7. Sample of $\text{CuCr}_2\text{S}_{3.5}\text{Se}_{0.5}$. Energy of the fundamental absorption edge E_a determined from the maximum on the $n(E)$ curve as a function of the temperature.

the width of the forbidden gap begins in just this energy range of the incident light and that this edge has an intricate structure. At low energies the plots of $\alpha(E)$ exhibit a rise in α with increasing E , which is followed by a step and then by a sharp steady increase in α . The step is more pronounced at low temperatures and is replaced by a hump at $T > T_C$ (curve 3). The absorption band edge was determined from the maximum on the plots of $n(E)$ shown in this figure. The vertical arrows on the plots of $\alpha(E)$ point out the positions of these maxima. The horizontal arrows indicate the beginning of the sharp ascent of the $\alpha(E)$ curves. It is seen that the positions of both the vertical and horizontal arrows shift to higher energies as the temperature decreases.

Figure 7 shows the temperature dependence of the energy of the absorption band edge E_a determined from the maximum of $n(E)$ for the sample with $x=0.5$. It is seen that the absorption band edge undergoes a large blue shift of the order of 0.15 eV in the $130 \leq T \leq 410$ K temperature range and that the rate of this shift is greatest in the vicinity of the Curie point. The plot of $E_a(T)$ for the sample with $x=1$ has approximately the same character. The magnitude of the blue shift here is about 0.14 eV in the $130 \leq T \leq 360$ K temperature range.

The only previously known ferromagnetic semiconductor exhibiting a large blue absorption and shift associated with ferromagnetic ordering was CdCr_2S_4 .^{8,9} The second such compound was discovered in the present work.

5. ANTIFERRON STATES OF CHARGE CARRIERS IN SEMICONDUCTING SAMPLES OF THE $\text{CuCr}_2\text{S}_{4-x}\text{Se}_x$ SYSTEM

Nagaev⁴ gave an explanation for the large blue shift of the width of the forbidden gap in ferromagnetic semiconductors based on the assumption that interband $s-d$ exchange plays a dominant role in them. Interband $s-d$ exchange is generally weaker than $s-d$ exchange in the conduction band, although it is stronger than $s-d$ exchange

in the valence band. This is attributable to the fact that in magnetic semiconductors the conduction electrons move mainly from one magnetic cation to another, while the valence-band electrons move from one nonmagnetic anion to another. However, for some reason the $s-d$ exchange in the conduction band may be weaker (for example, if the conduction band appears as a result of the hybridization of states with opposite signs of the exchange integral with localized d electrons). Interband $s-d$ exchange causes virtual transitions of electrons from the valence band to the conduction band. The interaction between two energy terms is known to result in repulsion between them. Like intraband exchange, interband $s-d$ exchange is enhanced when ferromagnetic ordering is established. Therefore, the repulsion between the valence band and the conduction band caused by it becomes stronger, i.e., the gap between them increases. The blue shift of the forbidden gap width associated with ferromagnetic ordering should be observed in just such cases. Ferromagnetic semiconductors with a blue absorption edge shift have specific properties that differ sharply from the properties of magnetic semiconductors with a red absorption edge shift.

The fact that the bottom of the conduction band in the case under consideration descends when the ferromagnetic ordering is disrupted renders "antiferromagnetic" states of the conduction electrons in crystals with a blue shift possible, in principle. They are characterized by the fact that conduction electrons create regions with disrupted ferromagnetic ordering in a ferromagnet and stabilize these regions by being trapped in them. The superexchange energy expended to create the nonferromagnetic regions is compensated by lowering of the electronic energy, since such regions are potential wells for conduction electrons. Such nonferromagnetic regions can also form around defects. In this case the trapping of an electron around a donor (or a hole around an acceptor) is promoted by the electrostatic attraction of the electron to the donor (the hole to the acceptor) in addition to the $s-d(p-d)$ exchange.

Several experimental facts attest to the existence of antiferromagnetic microregions in ferromagnetic In- or Ga-doped CdCr_2S_4 . For example, microregions with disrupted ferromagnetic ordering were discovered in In- or Ga-doped CdCr_2S_4 using Cd^{2+} , Ga^{3+} , and In^{3+} NMR.¹¹ In the opinion of Méry, Veillet, and Le Dang,¹¹ this disruption of the ferromagnetic ordering is caused by the exchange interaction of a valence electron of an impurity with the $3d$ electrons of the Cr^{3+} ions surrounding it, since the spin density of this electron, which derives from the hyperfine interaction, is unusually high. Therefore, these microregions are essentially antiferromagnetic. The existence of antiferromagnetic microregions in $\text{CdCr}_2\text{S}_4:\text{Ga}$ and $\text{CdCr}_2\text{S}_4:\text{Ga}$ was confirmed by the discovery of lowering of their paramagnetic Curie point (without a change in T_C) and magnetic moment as the doping increases.¹² In fact, since θ_p is determined by the sum of the exchange interaction occurring in the crystal, the presence of antiferromagnetic microregions with disrupted ferromagnetic ordering should lower θ_p , since exchange is suppressed in these regions. The lack of a magnetic moment in the antiferromagnetic region diminishes the magnetic mo-

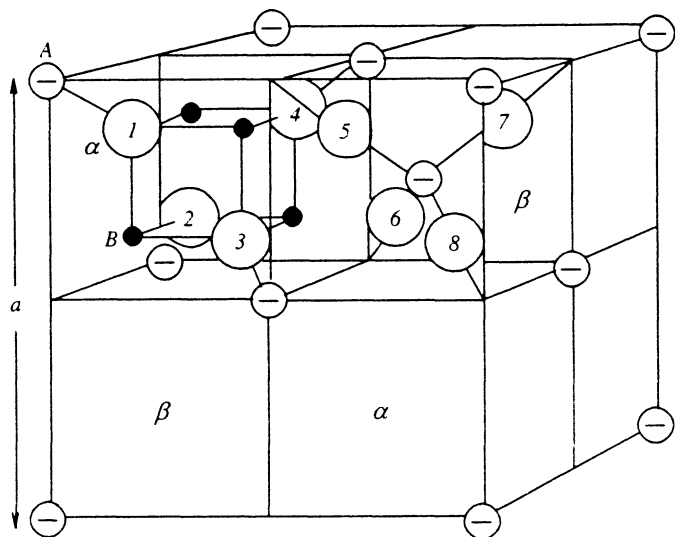


FIG. 8. Unit cell of a spinel structure: \circ —anions (chalcogen ions); \ominus —cations of A in tetrahedral sites; \bullet —cations of B in octahedral sites.

ment of the crystal as a whole. It should be noted that the lattice constant does not vary in response to doping of the type indicated and is equal to the lattice constant of the undoped compound, i.e., there are no variations in the exchange interactions due to variation of the lattice constant.

It was shown in Ref. 13 that the presence of two kinds of anions in a $\text{CdCr}_2\text{S}_{4-x}\text{Se}_x$ lattice results in a sharp decrease in the intraband s - d exchange constant. It is completely possible that a similar phenomenon also occurs in the $\text{CuCr}_2\text{S}_{4-x}\text{Se}_x$ system. This permits the existence of antiferromagnetic states in this system, whose presence can account for the semiconductor type of conduction and the lowering of the Curie temperatures and the magnetic moments in the samples with $0.5 \leq x \leq 1.5$ in comparison with the extreme compounds and the samples with $x \geq 2$. The samples with $x=0$ and $x \geq 2$ exhibit higher Curie points and a metallic type of conduction. It is assumed that in the samples with metallic conduction, whose data are presented in Table I, there is exchange by means of the charge carriers with resultant significant raising of the Curie points in comparison with the semiconducting ferromagnetic chalcogenide spinels, such as CdCr_2Se_4 , where $T_C = 130$ K. Trapping of the charge carriers in antiferromagnetic microregions produces semiconductor conduction in the samples with $0.5 \leq x \leq 1.5$. Due to the sharp decrease in the concentration of charge carriers (Fig. 3), exchange by means of the charge carriers is suppressed with the resultant lowering of T_C and θ_p . Since there is no magnetic moment in antiferromagnets, the total magnetic moment in the crystal is also lower than in the metallic samples of this system. The samples with $0.5 \leq x \leq 1.5$ are also characterized by anomalous relative positions for the ferro- and paramagnetic Curie points ($T_C > \theta_p$). It is also interesting that the magnetic moment n_p calculated for these samples from the Curie constant and the Curie-Weiss law is significantly higher than the magnetic moment at 4.2 K ($n_{4.2\text{K}}$). For $x \geq 2$ and $x=0$, on the other hand, $n_p < n_{4.2\text{K}}$ (Fig. 1 and Table I). Ferromagnets usually satisfy the relation $n_p < n_{4.2\text{K}}$, which is generally attributed to the temperature dependence of the exchange interactions. The unusual re-

lationship between n_p and $n_{4.2\text{K}}$ for the semiconducting samples can be explained in the following manner. The value of n_p is determined from data on the paramagnetic susceptibility at temperatures above T_C . At such temperatures the antiferromagnetic states are thermally destroyed in part, i.e., the lowering of the magnetic moment of the crystal as a whole, which can be observed, for example, at 4.2 K, decreases on their account. Since the paramagnetic Curie point is determined by the sum of the exchange interactions in the crystal, the contribution to the total exchange from the antiferromagnetic microregions, where ferromagnetic exchange is disrupted, lowers θ_p . At the same time, T_C is determined mainly by the connected ferromagnetic phase of the crystal, and therefore $T_C > \theta_p$.

Scattering by the magnetic moments of ferrons is known to be one of the causes of the maxima of ρ and the large negative magnetoresistance in the vicinity of T_C in magnetic semiconductors with a red shift of the absorption edge.¹⁴ Since antiferromagnets do not have a magnetic moment, these anomalies of the electrical properties in the vicinity of T_C should not be observed in the ferromagnetic semiconductors under consideration with a blue shift of the fundamental absorption edge. In fact, the measurements performed show that the value of $\Delta\rho/\rho$ is extremely small for the samples with $0.5 \leq x \leq 1.5$ and there is no maximum of ρ in the vicinity of T_C .

The mechanism for the formation of antiferromagnets in these solid solutions can be described in the following manner. Se^{2-} anions are known to be less electronegative than S^{2-} anions; therefore, an electron can pass from Se^{2-} to a sulfur atom and then from the S^- ion to a Cu^{2+} ion to form a Cu^{1+} ion. This process is equivalent to the capture of a hole by a selenium ion. Thus, the selenium ions in these solid solutions can serve as traps for holes. This hypothesis was advanced by van Stapele.¹⁵ Figure 8 shows the unit cell of a spinel structure. It shows the cations and anions for only one molecule of a given $\text{Cu}_2\text{Cr}_4\text{S}_{8-2x}\text{Se}_{2x}$ compound consisting of crystallographically inequivalent α and β octants. Four such molecules actually appear in the unit cell. Here the large unfilled circles represent the

TABLE II. Distribution of selenium ions in α and β octants of the spinel structure when antiferromicroregions are present in the α octants around selenium ions.

No		Composition, x		0.5	1.0	1.5
1	one selenium ion found in each α octant and forming an antiferromicroregion from three nearest-neighbor Cr^{3+} ions	distribution of selenium ions among octants, %	α with one	100	50	33.3
			α with two	0	0	0
		magnet moment per chemical formula unit μ_B	β	0	50	66.6
			calculated	0.83	0.83	0.83
2	maximum number of selenium ions found in α octants with 2 selenium ions and forming an antiferromicroregion from four Cr^{3+} ions	distribution of selenium ions among octants, %	observed $n_{4,2K}$	1.9	0.75	1.8
			α with one	0	0	0
		number of α octants not containing selenium, %	α with two	100	100	66.7
			β	0	0	33.3
magnetic moment per chemical formula unit, μ_B	calculated	2.16	0	0		
	observed	1.9	0.75	1.8		
3	some selenium ions found in α octants with 1 selenium ion and forming antiferromicroregions, the calculated magnetic moment being equal to $n_{4,2K}$ observed	distribution of selenium ions among octants, %	α with one	69.3	not determinable	24.1
			α with two	0	not determinable	0
		number of α octants not containing selenium, %	β	30.7	not determinable	75.9
				30.7	not determinable	27.8
4	maximum number of α octants with 1 and 2 selenium ions forming antiferromicroregions from four Cr^{3+} ions, the calculated magnetic moment being equal to $n_{4,2K}$ observed	distribution of selenium ions among octants, %	α with one	19.5	47.5	9
			α with two	80.5	5	24.3
		number of α octants not containing selenium, %	β	0	47.5	66.7
				40.3	0	36.5
5	some selenium ions found in α octants with 2 selenium ions, the calculated magnetic moment being equal to $n_{4,2K}$ observed	distribution of selenium ions among octants, %	α with one	not determinable	0	0
			α with two	not determinable	82.6	39
		number of α octants not containing selenium, %	β	not determinable	17.4	61
				not determinable	17.4	41.6

chalcogen anions, the hatched circles represent the copper cations in the A sites, and the filled circles represent the Cr^{3+} cations in the B sites.

A hole p originating from a copper ion can be trapped near a selenium ion, disrupting the ferromagnetic ordering among the Cr^{3+} ions near it and forming an antiferromicroregion. As is seen from Fig. 8, the Cr^{3+} ions are concentrated in the four α octants and are absent from the four remaining β octants. Therefore, the formation of antiferromicroregions is possible only in the α octants. The magnitude of the magnetic moment is clearly dependent on the distribution of the Se^{2-} ions among the α and β octants. The results of calculations of the magnetic moment or semiconducting samples are presented in Table II. Here we consider five kinds of distributions for which this calculation is possible.

1. One selenium ion appears in each α octant and forms an antiferromicroregion from the three nearest-neighbor Cr^{3+} ions in it. The resultant magnetic moment per molecule is calculated in the following manner. In CuCr_2S_4 the magnetic moment is known to be created by the ferromagnetically ordered magnetic moments of the chromium ions and the magnetic moments of the collective holes that are antiparallel to them (there is one hole for every two Cr^{3+} ions). The magnetic moment of two Cr^{3+} ions is clearly equal to the sum of the magnetic moments in CuCr_2S_4 ($4.32 \mu_B$ from Table I) and $-1\mu_B$, i.e., $5.32 \mu_B$. Thus, there is $2.66 \mu_B$ for each Cr^{3+} ion. In this case the mag-

netic moment discovered when an Se ion is introduced into position 1, 2, 3, or 4 in Fig. 8 with the formation of an antiferromicroregion involving the three nearest-neighbor Cr^{3+} ions is equal to $(2.66 \mu_B) \cdot 3 - 1\mu_B = 6.98 \mu_B$ (the magnetic moment of a hole equal to $-1 \mu_B$ is taken into account here). In this case the magnetic moment of one Cr^{3+} ion and the magnetic moment of one hole, which are generally antiparallel, participate in the magnetic ordering of the crystal, i.e., the magnetic moment per molecule should be equal to $1.66 \mu_B$ and the magnetic moment per chemical formula unit should be $0.83 \mu_B$. A comparison of this magnetic moment with the empirical value (Table II) reveals that they differ strongly for all the semiconducting samples. This disparity can be eliminated by assuming that only some of the selenium ions, say y atoms, appear in the α octants and form antiferromicroregions, while $1-y$ Se^{2-} ions appear in the β octants, where there are no Cr^{3+} ions and the formation of antiferromicroregions is impossible. Such a distribution is considered in paragraph 3.

2. The maximum number of selenium ions appears in the α octants, i.e., two in each octant, and they form an antiferromicroregion from four Cr^{3+} ions. As is seen from Fig. 8, in this case all four Cr^{3+} ions are nearest neighbors of the selenium ions, and two holes trapped by the selenium ions form one antiferromicroregion from them. In the sample with $x=0.5$ such an antiferromicroregion forms in half of all the molecules, and in the samples with $x=1.0$ and 1.5 such an antiferromicroregion forms in all the molecules. The magnetic moments of the last two

samples are equal to zero in this case, and the magnetic moment of the first sample is equal to half of the magnetic moment of a molecule not containing selenium (the magnetic moment of the latter is clearly equal to twice the magnetic moment of CuCr_2S_4 , i.e., $8.64 \mu_B$). Thus, the magnetic moment per chemical formula unit for the sample with $x=0.5$ equals $2.16 \mu_B$. As is seen from Table II, none of the magnetic moments calculated in this paragraph for the semiconducting samples correspond to the empirical values. The next three paragraphs describe methods for fitting the magnetic moments calculated for different distributions of the selenium ions to the empirical values.

3. Some of the selenium ions (y) appear as the only such ion in α octants and form antiferromagnets, the value of y being such that the calculated magnetic moment is equal to the observed value. In this case the magnetic moments of $(4-3y)\text{Cr}^{3+}$ ions per molecule and the magnetic moments of $(2-y)$ holes, which are antiparallel to them, participate in the magnetic ordering of the crystal. Setting, as before, the magnetic moment of Cr^{3+} equal to $2.66 \mu_B$ and the magnetic moment of a hole equal to $-1\mu_B$, we can use the equation

$$(4-3y)2.66 - (2-y)1 = 2n_{4.2K} \quad (2)$$

to find y . As is seen from Table II, $y=0.693$ for the sample with $x=0.5$. Thus, the empirical magnetic moment $n_{4.2K}=1.9 \mu_B$ for the sample with $x=0.5$ can be attributed to the formation of antiferromagnets from three Cr^{3+} ions around a selenium ion occupying position 1, 2, 3, or 4 in an α octant. Here 69.3% of the selenium ions occupy such positions, and 30.7% occupy positions in the β octants, in which the formation of antiferromagnets is impossible. The decrease in the number of selenium ions in the α octants upon the transition from distribution 1 to distribution 3 increases the magnetic moment, while for the sample with $x=1$ it must be decreased to achieve a fit to the experimental value. Therefore, the fitting method described in this paragraph is inapplicable to the sample with $x=1.0$. The results of such fitting for the sample with $x=1.5$ are presented in Table II.

4. The maximum number of α octants contain selenium ions: y ions appear in octants containing one such ion, and $(1-y)$ ions appear in octants containing two such ions, the value of y being such that the calculated magnetic moment is equal to the observed value. Clearly, for the sample with $x=0.5$, $(1-y)/2$ α octants do not contain selenium ions, and their contribution to the magnetic moment per molecule is equal to twice the magnetic moment of CuCr_2S_4 multiplied by $(1-y)/2$. The contribution from the octants containing antiferromagnets consisting of three Cr^{3+} ions is equal to $(2.66y-1y)\mu_B$. The value of y corresponding to the experimentally determined magnetic moment is found from the following equation:

$$1.66y + 4.32(1-y) = 2n_{4.2K} \quad (3)$$

Substituting $n_{4.2K}=1.9$ into this equation, we obtain $y=0.195$. This means that 19.5% of the selenium ions appear in α octants containing one such atom, 80.5% of them appear in α octants containing two such atoms, and 40.3%

of the α octants do not contain selenium. The low value of $n_{4.2K}$ for the sample with $x=1$ permits realization of a case in which there are no α octants without antiferromagnets and the magnetic moment is determined only by the contribution from the α octants containing antiferromagnets consisting of three Cr^{3+} ions. The value of y is determined from

$$1.66 = 2n_{4.2K} \quad (4)$$

The results of fitting the samples with $x=1$ and 1.5 are presented in Table II.

5. Some y molecules have two selenium ions in an α octant and do not have a magnetic moment, while the other $(1-y)$ molecules do not contain selenium ions and have a magnetic moment equal to $8.64 \mu_B/\text{molecule}$, the value of y being such that calculated magnetic moment is equal to the observed value. In this case y is found from

$$(1-y)8.64 = 2n_{4.2K} \quad (5)$$

For the sample with $x=0.5$, $y=0.56$. This means that 56% of the α octants contain two selenium ions; however, as is seen from paragraph 2 and Table II, in the sample with $x=0.5$ these octants can amount to no more than 50%. Therefore, such a distribution is impossible for this sample. The results of fitting the samples with $x=1$ and 1.5 are presented in Table II.

Charge carriers are trapped in the antiferromagnetic microregions; therefore, conduction occurs in the crystal along the α octants not containing selenium ions, as well as along the β octants. If these regions are connected in a single system, a metallic type of conduction should be observed, as in CuCr_2S_4 and CuCr_2Se_4 . Therefore, of the adjustable distributions just described, the distributions having the fewest α octants without selenium ions are most suitable. Table II reveals that distribution 3 satisfies this criterion for the samples with $x=0.5$ and 1.5 and that distribution 4 satisfies it for the sample with $x=1$. Then the filling of the α and β octants with selenium ions conforms to the following picture. In the sample with $x=0.5$, 69.3% of all the selenium ions are in α octants, and 30.7% are in β octants. In the sample with $x=1$ there are twice as many selenium ions than in the preceding sample, and they occupy all the α octants (90.5% of the α octants contain one selenium ion and 9.5% contain two selenium ions). In this case 52.5% of the selenium ions are located in α octants, and 47.5% are found in β octants. In the sample with $x=1.5$, 72.2% of the α octants are occupied by one selenium ion, or 24.1% of the selenium ions are in α octants and 75.9% are in β octants. Thus, as sulfur is replaced by selenium in the system under consideration, at first the α octants are occupied (one or two ions per octant) to a greater degree than are the β octants, in the sample with $x=1$ the numbers of selenium ions in the α and β octants are almost equal, and in the sample with $x=1.5$ the filling of the β octants already predominates. In general, distribution 5 for the sample with $x=1$ also corresponds to the criterion indicated above. However, under this distribution 82.6% of the selenium ions are found in α octants, and 17.4% are found in β octants. This contradicts the conclusion in Ref. 16, in which the ordering between the sulfur and selenium

ions in the anion sublattice was established for the sample with $x=1$ from x-ray diffraction data. The data in Ref. 16 are clearly in better agreement with distribution 4 for this sample.

As is seen from Table I, for the samples with $2 \leq x \leq 3.5$ the value of the magnetic moment ($n_{4.2K} \geq 4.8 \mu_B$) is very close to $n_{4.2K} = 5.08 \mu_B$ for CuCr_2Se_4 , and they exhibit a metallic type of conduction. This means that an antiferromagnetic effect is not realized in them. Here we should recall the work in Ref. 17, where the ^{53}Cr NMR spectra of samples with $1.75 \leq x \leq 4$ revealed that a statistical distribution of S and Se is observed only for the samples with $3 \leq x \leq 4$, while the existence of two groups of anionic octahedrons formed mainly by sulfur or selenium around Cr^{3+} ions should be postulated for the other samples investigated.

Some other possible causes of the observed anomalies in the electrical and magnetic properties of the system under consideration should be discussed. According to Berdyshev,¹⁸ when a continuous ferromagnetic system is formed, the passage of electrons not only between cations, but also between anions is possible. The Se^{2-} anion is less electronegative than the S^{2-} anion; therefore, an electron can pass from Se^{2-} to S^{2-} with the resultant appearance of an excited configuration of anions. When such an excited configuration exists, passage of an electron from an anion to an unoccupied orbital of a cation is possible. If this electron enters a chromium 3d level and a chromium ion becomes divalent, the magnetic moment of the compound should decrease in the low-spin configuration. However, such an explanation provides a drop in the magnetic moment that is considerably smaller than the experimentally observed decrease. Here the magnetic moment can decrease by no more than $1 \mu_B$ for every selenium ion introduced into the molecule, while in the same study the decrease for the sample with $x=0.5$ amounted to $4.84 \mu_B$ (instead of $1 \mu_B$), the decrease for the sample with $x=1$ amounted to $7.14 \mu_B$ (instead of $2 \mu_B$), and the decrease for the sample with $x=1.5$ amounted to $5.04 \mu_B$ (instead of $3 \mu_B$), i.e., the decrease in the magnetic moment was several times greater than the decrease predicted under the hypothesis being discussed. Moreover, this hypothesis does not provide any explanation for the semiconductor type of conduction of the samples with $0.5 \leq x \leq 1.5$. Another possible cause for the appearance of semiconductor conduction in these samples is the scattering of charge carriers by lattice defects, but it cannot account for the anomalies in the magnetic properties indicated above.

Despite the approximate nature of the calculation performed above, the hypothesis that antiferromagnets form in the system is most suitable for explaining the anomalies in the magnetic and electrical properties.

6. CONCLUSIONS

The magnetic, electrical, and optical properties of the $\text{CuCr}_2\text{Sr}_{4-x}\text{Se}_x$ system, which consists of solid solutions of the two thoroughly studied chalcogenide spinels CuCr_2S_4 and CuCr_2Se_4 with a metallic type of conduction, have been studied. It has been found that the samples with $0.5 \leq x \leq 1.5$ have properties characteristic of semiconduc-

tors: the resistivity and the concentration of charge carriers decrease as the temperature rises, and the spectra of the absorption coefficient obtained from the diffuse reflectance spectra with the aid of the Kramers–Kronig relations display a pronounced fundamental absorption edge. In addition, in these samples the anomalous Hall effect is much smaller than in the metallic samples of this system, as is typical of magnetic semiconductors.⁵

The paramagnetic susceptibility of all the samples of this system obeys the Curie–Weiss law, and the paramagnetic Curie point θ_p for the semiconducting samples is below the Curie point T_C obtained by extrapolating the steepest part of the temperature dependence of the spontaneous magnetization. The magnetization isotherms of all the samples reach saturation in fields $H \leq 10$ kOe. The semiconducting samples exhibited sharp decreases in θ_p and T_C , as well as in the magnetic moment obtained from measurements of the magnetization at 4.2 K ($n_{4.2K}$) and from measurements of the paramagnetic susceptibility (n_p), relative to the extreme compounds, the inequalities $n_p > n_{4.2K}$ and $\theta_p > T_C$ being observed here. Although the Curie points of the semiconducting samples are lower than those of the extreme compounds, which have a metallic type of conduction, they are still above 300 K. Thus, new magnetic semiconductors with Curie points have room temperature were discovered in the present work.

It was discovered that the fundamental absorption edge of the semiconducting samples undergoes a large blue shift (~ 0.15 eV), which is associated with ferromagnetic ordering, and that the rate of this shift is greatest in the vicinity of T_C . The occurrence of this blue shift allows the existence of antiferromagnetic microregions with disrupted ferromagnetic ordering in the semiconducting samples. As was shown by Nagaev,⁴ the formation of such microregions, which are created by the self-trapping of charge carriers in them due to a gain in the energy of interband s – d exchange is possible in ferromagnetic semiconductors with a blue shift of the forbidden gap width.

In this research it was shown that the sharp decrease in magnetic moment in the semiconducting samples is attributable to the formation of antiferromagnets around selenium ions by three or four Cr^{3+} ions that are nearest neighbors of the selenium ions. The abrupt lowering of the Curie points in the semiconducting samples in comparison with the extreme compounds is attributed to the suppression of exchange through charge carriers in them due to the trapping of charge carriers (holes) in the antiferromagnetic microregions. As we know, ferromagnets are usually characterized by the relation $n_p < n_{4.2K}$, which is generally attributed to the temperature dependence of the exchange interactions. The usual relation between n_p and $n_{4.2K}$ for the semiconductor samples can be explained in the following manner. The magnetic moment n_p , is determined from data on the paramagnetic susceptibility at temperatures above T_C . At such temperatures the antiferromagnets are thermally destroyed in part, i.e., the lowering of the magnetic moment of the crystal as a whole, which can be observed, for example, at 4.2 K, decreases on their account. Since the paramagnetic Curie point is determined by the sum of the exchange in-

teractions in the crystal, the contribution to the total exchange from the antiferromicroregions, where ferromagnetic exchange is disrupted, lowers θ_p . At the same time, T_C is determined mainly by the connected ferromagnetic phase of the crystal, and therefore $T_C > \theta_p$.

In conclusion, we express our thanks to I. V. Gordeev and V. A. Alferov for preparing the samples and analyzing them.

- ¹K. P. Belov, Yu. D. Tret'yakov, I. V. Gordeev *et al.*, *Magnetic Semiconductors-Chalcogenide Spinels* [in Russian], Izd. MGU, Moscow (1981), p. 279.
- ²L. I. Koroleva and M. A. Shalimova, *Fiz. Tverd. Tela* (Leningrad **21**, 449 (1979) [Sov. Phys. Solid State **21**, 266 (1979)]).
- ³L. I. Koroleva, V. Yu. Pavlov, and N. Yu. Rylova, *Fiz. Tverd. Tela* (Leningrad **26**, 1859 (1984) [Sov. Phys. Solid State **26**, 1126 (1984)]).
- ⁴É. L. Nagaev, *Pis'ma Zh. Eksp. Teor. Fiz.* **25**, 87 (1977) *JETP Lett.* **25**, 76 (1977).
- ⁵É. L. Nagaev and É. B. Sokolova, *Fiz. Tverd. Tela* (Leningrad), **19**, 732 (1977) [Sov. Phys. Solid State **19**, 425 (1977)].
- ⁶L. I. Koroleva, Sh. Z. Sadykova, and V. Yu. Pavlov, *Fiz. Tverd. Tela*

(St. Petersburg) **34**, 3638 (1992) [Sov. Phys. Solid State **34**, 1948 (1992)].

- ⁷R. K. Ahrenkiel, *J. Opt. Soc. Am.* **61**, 1651 (1971).
- ⁸G. Harbeke and H. Pinch, *Phys. Rev. Lett.* **17**, 1090 (1966).
- ⁹S. B. Berger and L. Ekstrom, *Phys. Rev. Lett.* **23**, 1499 (1969).
- ¹⁰B. Velický, *Czech. J. Phys.* **B11**, 787 (1961).
- ¹¹M. C. Méry, P. Veillet, and K. Le Dang, *Phys. Rev. B* **31**, 2656 (1985).
- ¹²K. P. Belov, S. D. Batorova, L. I. Koroleva *et al.*, *Pis'ma Zh. Eksp. Teor. Fiz.* **26**, 68 (1977) *JETP Lett.* **26**, 62 (1977).
- ¹³Z. É. Kin'kova, T. G. Aminov, and L. L. Golik, *Fiz. Tverd. Tela* (Leningrad) **18**, 2083 (1976) [Sov. Phys. Solid State **18**, 1212 (1976)].
- ¹⁴É. L. Nagaev, *Physics of Magnetic Semiconductors* [in Russian], Nauka, Moscow (1979), p. 431.
- ¹⁵R. P. van Staple, "Sulphospinel," in *Ferromagnetic Materials*, North-Holland (1982), Vol. 3, p. 603.
- ¹⁶K. Ohbayashi, Y. Tominaga, and S. Iida, *J. Phys. Soc. Jpn.* **24**, 1173 (1968).
- ¹⁷H. Figiel, J. Kukucz, and A. Bombik, *J. Magn. Magn. Mat.* **15-18**, 701 (1980).
- ¹⁸A. A. Berdyshev and A. A. Sidorov, *Uch. Zap. Ural. Gos. Univ.* **43** (1969).

Translated by P. Shelnitz